

# RF-MEMS Switching Concepts for High Power Applications

Karl M. Strohm, Bernd Schauwecker, Dietmar Pilz\*, Winfried Simon<sup>#</sup>,  
Johann-Friedrich Luy

DaimlerChrysler Research Center Ulm, Wilhelm Runge Straße 11, 89081 Ulm, Germany  
Tel.: (49) 731 505 2025, Fax: (49) 731 505 4102, E-mail:karl.strohm@daimlerchrysler.com

\*DaimlerChrysler Aerospace, Wörthstraße 85, 89077 Ulm, Germany

<sup>#</sup>IMST GmbH, Carl-Friedrich-Gauß-Str. 2, 47475 Kamp-Lintfort

## Abstract

RF MEMS switches for power applications are discussed and mechanical and electromagnetic simulations of a new switch type for power applications are presented and fabrication aspects are discussed.

## Introduction

Over the past several years, developments in Micro-Electro-Mechanical Systems (MEMS) have promoted exciting advancements in the field of microwave switching. Micromechanical switches were first demonstrated in 1971 [1] as electrostatically actuated cantilever arms used to switch low-frequency electrical signals. Since then, these switches have demonstrated useful performance at microwave frequencies. Different switch topologies have been investigated and tested [2, 3], and most of them use electrostatic actuation. The advantage of using MEMS over conventional solid state switching devices such as FETs or p-i-n diodes is their low loss performance, low power consumption and lack of measurable intermodulation distortion. There are three main challenging aspects for RF MEMS switches: lowering the actuation voltage, increasing the switching speed and increasing power handling capabilities. For lowering the switching speed meander spring suspension [4] and push-pull concepts have been investigated [5]. Increasing the switching speed and the power handling capabilities are still a problem. DaimlerChrysler has developed capacitive RF shunt switches with gold metallization lines and gold membranes [6]. Using these capacitive RF shunt switches a 180° phase shifter has been realized [7]. DaimlerChrysler is now developing RF MEMS SPDT switches for RF power application beyond 10 W. For this, new switching concepts are evaluated.

## Power handling capabilities

The power handling capabilities of the RF MEMS switches can be limited either by the current density on the transmission lines causing excessive heating or by the actuation of the switches due to the average RF-voltage on the coplanar waveguide (CPW) line (denoted as "self biasing"). Since the electrostatic force acting on the switch can derive either from a negative or positive voltage, and since the relaxation time of free electrons in metals is in the range of  $10^{-14}$  s ( for Au:  $\tau_{Au} = 2.9 \cdot 10^{-14}$  s, for Al:  $\tau_{Al} = 0.8 \cdot 10^{-14}$  s ) which corresponds to frequencies of 100 THz, the electrostatic force instantaneously follows the applied high

frequency electromagnetic field. Thus the average voltage level of the rectified sine wave due to the RF power on the CPW line is attracting the switch. The following simple calculation may be performed:

$$P = UI = \frac{U_{\text{eff}}^2}{R} = \frac{U_0^2}{2R}$$

$$U_0 = \sqrt{2RP} = \sqrt{2 \cdot 50 \text{ Ohm} \cdot 10 \text{ Watt}} = 31 \text{ Volt}$$

with  $U_{\text{eff}} = \frac{U_0}{\sqrt{2}}$   
 $R = 50 \ \Omega$

Using a 50 Ω line and an RF power of 10 Watt results in a maximum voltage U<sub>0</sub> of 31 V. Allowing a pull-down voltage of 50V results in a maximum power of 25 W.

However, power data have rarely been reported in literature, primarily because the test set-up requires a relatively expensive high-power RF generator. The following data are reported: Brown [2] mentions in his review article a private communication from J. Goldsmith (Raytheon) that self-closing is observed with approximately 3 W CW power at 10 GHz and with approximately 1 W at 35 GHz. Pacheco [5] reports on capacitive shunt switches no "self biasing" or failure of the RF MEMS switches for power levels up to 6.6 W in the X-band (10 GHz). Schaffner [8] reports on resistive cantilever switches power switching up to 1 Ω in a 50 Ω line. Our investigations show that self switching may occur.

In Fig. 1a self switching is measured for a non-optimized capacitive shunt switch at 0.96 W at 35 GHz. However, for optimized switches no self closing is observed up to 1 Watt at 35 GHz, which was the limit of the power amplifier (see Fig. 1b).

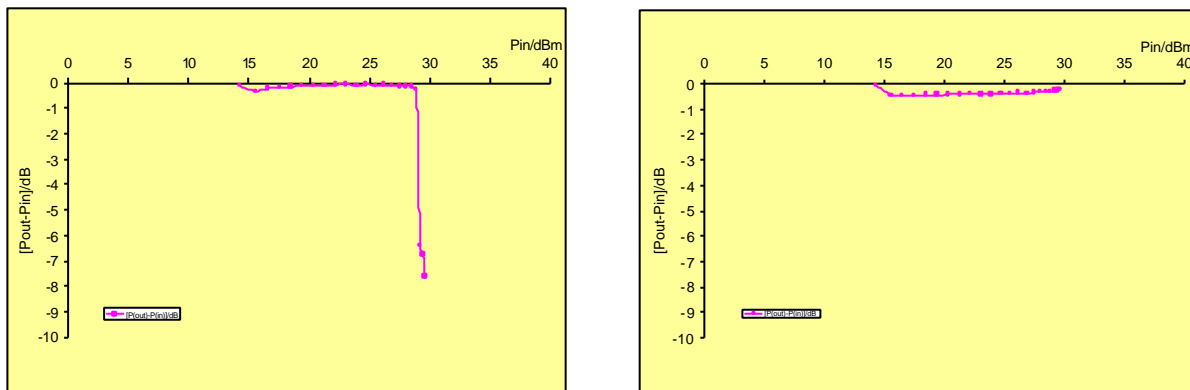


Fig.1: a) self closing of a non-optimized capacitive RF shunt switch at 35 GHz      b) power measurement of an optimized capacitive shunt switch at 35 GHz

These results indicate that for power beyond 10 Watt new switching concepts have to be investigated.

### The new switch concept

The proposed concept is a so called "double anchor switch" (Fig. 2). The double anchor switch consists of two fixed electrodes: a bottom electrode and a top electrode. The switching membrane in this case is fixed at both ends and can be actuated either to the bottom or top electrode. Therefore self closing due to RF power should be strongly reduced.

This switch type is also very suited for SPDT switches, since one can switch from input port 1 (membrane) to output port 2 (connected to bottom electrode) or to output port 3 (connected to top electrode), shown in Fig. 2.

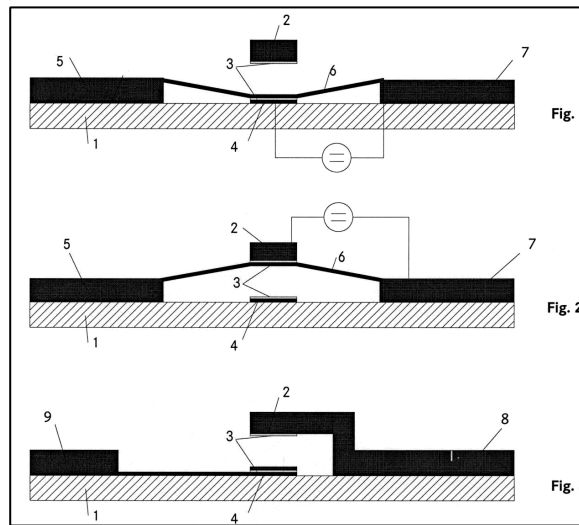


Fig. 2: Schematic concept of a so called "double anchor switch"

Another type of the double anchor switch consists of one flexible membrane fixed only at one end, which can be switched up and down (Fig.3). In the down position the signal is routed to port 3 and in the up position is the signal routed with a 90° bend to port 2, as depicted in Fig. 3 and 4. Also, this type of switch is suitable for an SPDT switch.

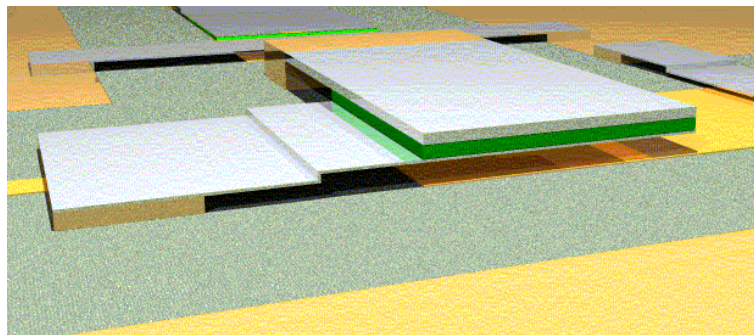


Fig. 3: Schematic concept of an STDT switch by using a double anchor switch

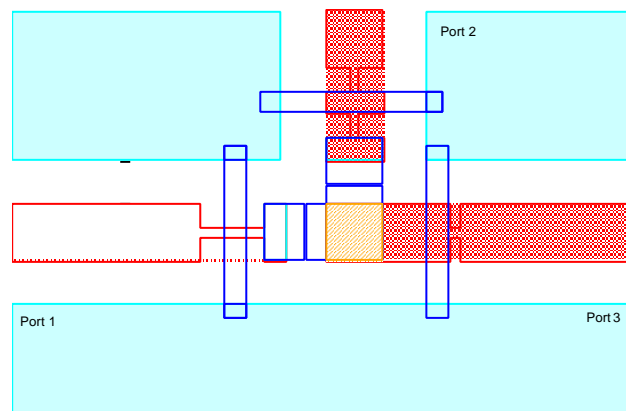


Fig.4 Schematic / layout view of the double anchor switch in SPDT operation

## Electromagnetic simulation

Different SPDT switch topologies have been simulated. One topology was with two Serial-Air-Bridge MEMS switches. In comparison to this the scattering capacitance of an SPDT switch with a single-ended "double anchor switch" is lower, because there is no open end stub in case of routing the signal to port 2. This yields better results in return loss and insertion loss if the signal is switched to port 2. The air bridges at the bend (see Fig. 4) are necessary to suppress asymmetrical modes on the coplanar line to port 2. In Fig. 5, the simulated S-parameter for the on-state and off-state for the different paths are depicted. For thru to port 2 the insertion loss  $S_{21}$  is -0.06 at 8 GHz and -0.7 dB at 30 GHz. Isolation to port 3 ( $S_{31}$ ) is -34.7 dB at 8 GHz and -17.3 dB at 30 GHz. For thru to port 3 the insertion loss  $S_{31}$  is -0.18dB at 8 GHz and -0.47dB at 30 GHz. Isolation to port 2 ( $S_{21}$ ) is -32dB at 8 GHz and -16 dB at 30 GHz. For the simulations no metallic losses have been taken into account. Investigations have shown, that metallic losses for the used CPW lines are less than 0.1 dB at 30GHz. Since the isolation decreases with increasing frequency additional shunt capacitive switches may be used for improved SPDT switches.

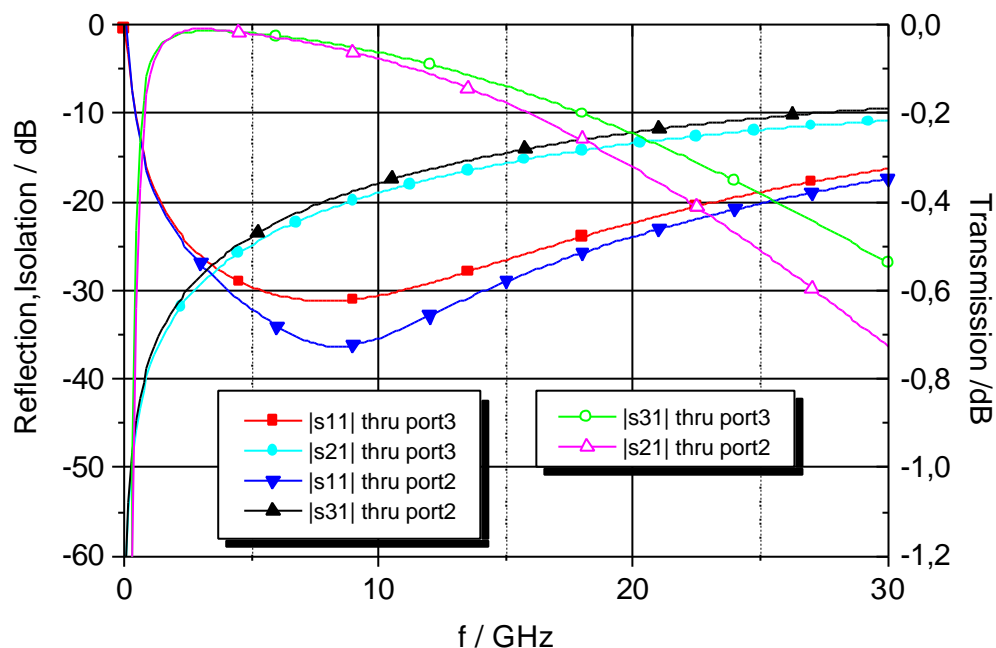


Fig.5: Simulation results of the SPDT build from double anchor switches (open/closed) position

## Mechanical simulation

In addition to the electromagnetic simulation, mechanical simulations of the new structure are performed. The membrane is in the middle of two fixed electrodes and consists of aluminum or gold with a thickness between 0.75  $\mu\text{m}$  and 1  $\mu\text{m}$ . The distance between lower and upper electrodes is 6  $\mu\text{m}$ , and between membrane and electrodes is 3  $\mu\text{m}$ . A thin dielectric film is deposited both over and under the electrodes. A schematic view of the simulated structure is shown in Fig. 6.

Due to the small membrane thickness the mechanical structure was simulated with the simulation program ANSYS. The structure was described with dish elements. With these simulations the actuation voltage and the stress distribution in the actuated membrane (membrane in contact) are calculated. The behavior of the membrane is simulated with the flexure line as an analytical function and with the energy at equilibrium. The gravitation force

can be neglected. In Fig. 7, the stress distribution is shown for a gold-membrane when it is in full contact to an electrode area. Red color indicates the tensile stress (positive sign) and blue color indicate the compressive stress (negative sign).

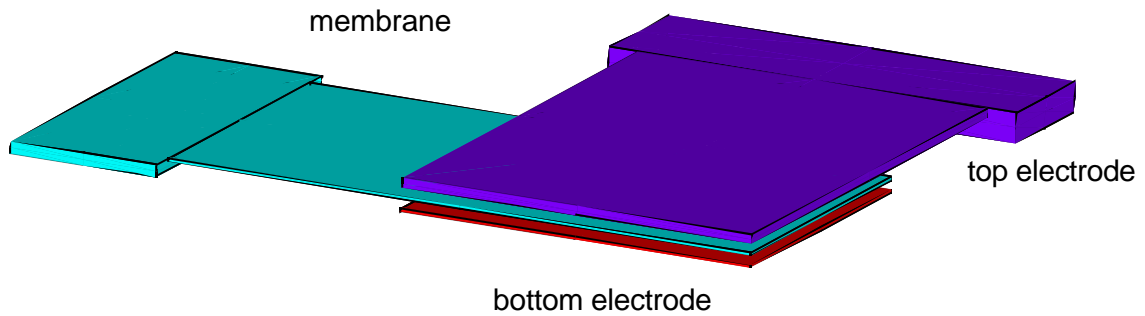


Fig. 6: Schematic view of the double anchor structure for mechanical simulation

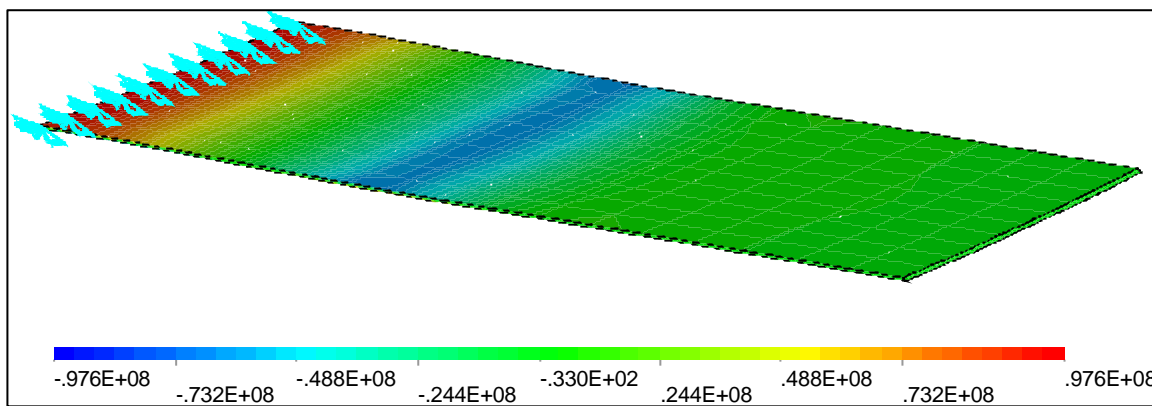


Fig. 7: Stress distribution in the membrane when contacted with an electrode (Units are Pa)

The calculated stress in the membrane is less than 50 MPa at the fix point. The simulated actuation voltages are in the range between 4 V and 14 V. The resonance frequencies for this structure are in the range from 6 kHz to 21 kHz.

### Fabrication process

The capacitive RF switches are fabricated on high-resistivity silicon wafers ( $\rho > 4000 \Omega\text{cm}$ ) with a wafer thickness of 525  $\mu\text{m}$ . The fabrication process of a capacitive RF switch is depicted in Fig. 8.

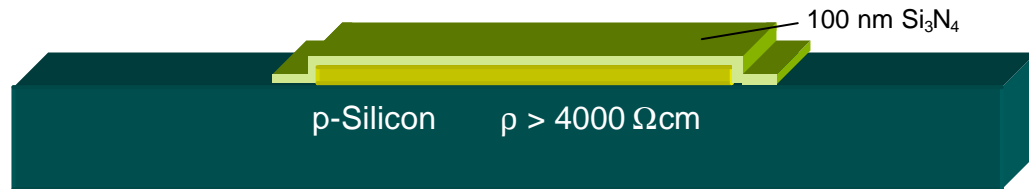
First, the lower electrode (underpass metallization) is defined by a lift-off process with 50 nm Ti and 300 nm Au. Then, the lower electrode is isolated by a 100 nm thick PECVD silicon nitride layer under the membrane region. Next, the transmission lines are defined by a lift-off process with 50 nm Ti and 2500 nm Au. At this point, an air-bridge resist with a height of 2.5-3  $\mu\text{m}$  is patterned as sacrificial layer. Afterwards, the membrane metallization is sputtered. The membrane material consists of 0.5-1  $\mu\text{m}$  Au or Al. Lastly, the membrane resist is defined and the membrane is etched.

After these steps, a third electrode on top must be defined. For this, an air-bridge resist with an height of 2.5-3  $\mu\text{m}$  is patterned as second sacrificial layer. Then, the third upper electrode is isolated by a 100 nm PECVD silicon nitride layer over the resist and under the region of the third electrode. Next, the metallization for the third electrode is sputtered. The electrode

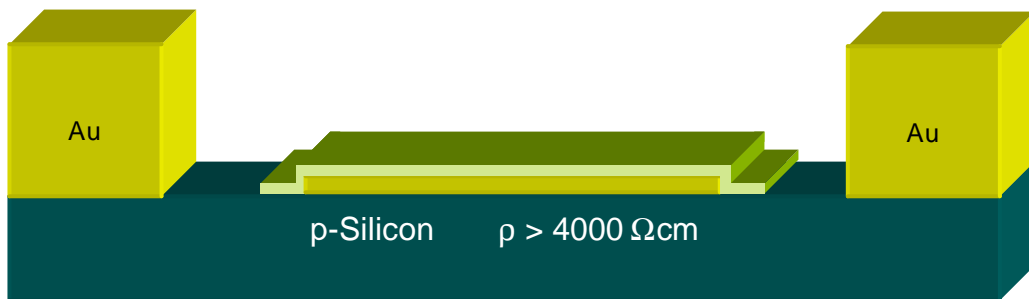
material consists of 1-2  $\mu\text{m}$  Au. Here, the third electrode resist is defined and the electrode material is etched. Finally, the membrane resist and the two air-bridge resists are removed.



(1) Lower electrode (underpass – metallization): 50 nm Ti, 300 nm Au



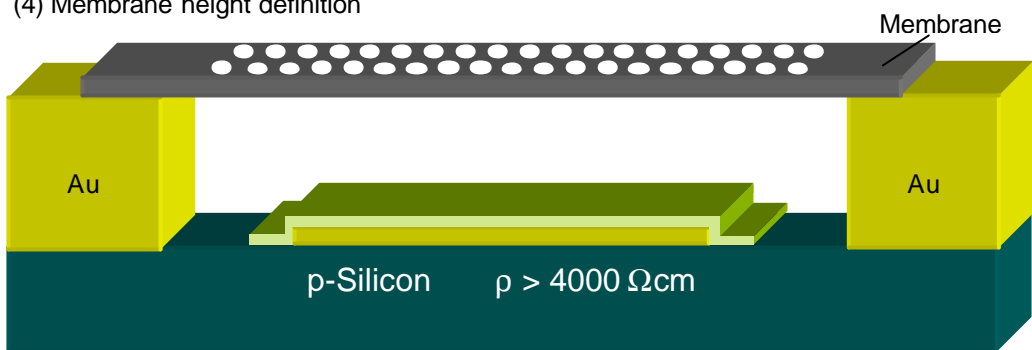
(2) Isolation layer for lower electrode: 100 nm  $\text{Si}_3\text{N}_4$



(3) Definition of the transmission lines: 50 nm Ti, 2500 nm Au



(4) Membrane height definition



(5) Membrane definition

Fig. 8: Fabrication process of the switch membrane (two electrodes)

Stiction is a difficulty in the fabrication process. When the wafer is pulled out of the rising solution used to dissolve the sacrificial layer (photoresist in our case) sticking of the structural elements to the substrate may occur [10]. This can be avoided by supercritical  $\text{CO}_2$  drying [9]

or vapor phase etching. In our case, the sacrificial photoresist layers are removed in  $O_2$  plasma. Fig. 9 shows the layout of a capacitive RF membrane switch chip with 120  $\mu\text{m}$  signal line and 90  $\mu\text{m}$  spacing (6 times scaling of our standard 50  $\Omega$  CPW lines). The width of the membrane is 100  $\mu\text{m}$ , the distance of the membrane to the enforced transmission signal line is 15  $\mu\text{m}$ . The total chip size is 1300  $\mu\text{m}$  x 1100  $\mu\text{m}$ , and the metallized chip size is 1200  $\mu\text{m}$  x 1000  $\mu\text{m}$ .

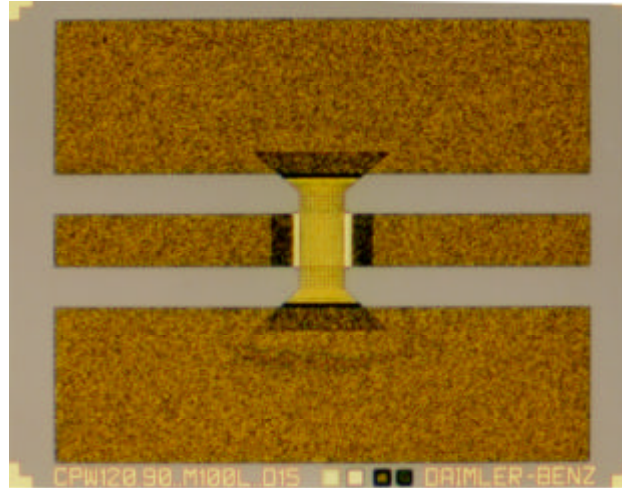


Fig. 9: Micrograph (layout) of a capacitive RF switch chip

The membrane metallization thickness was 1  $\mu\text{m}$ , the height above ground was 3.3  $\mu\text{m}$  and the transmission line metallization thickness was 3.6  $\mu\text{m}$ .

The pull-in voltage for the measured switch is 25 V. The pull-in voltage ranges from 25 V to 50 V, depending on membrane thickness, membrane height and fabrication process. Insertion loss lower than 0.3 dB @ 35GHz in the off-state (0 V) and isolation down to 35 dB @ 35 GHz in the on-state (25 V) are measured.

## Conclusion

A new capacitive SPDT switch for power applications is proposed. The electrical and mechanical properties and behaviors of this so called "double anchor switch" are discussed. Also, technology fabrication aspects of the new switch type are discussed. Capacitive RF-switches have already been fabricated on high resistivity silicon substrates. Measurements demonstrate that these metallic membrane switches have low insertion loss and a good isolation at frequencies into the millimeter-wave bands. These devices offer the potential for building a new generation of low loss high linearity microwave circuits for a variety of phased antenna arrays radar and communication applications.

## Acknowledgement

The authors would like to acknowledge A. Lauer and A. Wien (IMST GmbH, Kamp-Lintfort) for the electrical simulations as well as J. Mehner (FEM ware GmbH) for mechanical simulations.

## References:

- [1] K. E. Petersen, "Micromechanical Switches on Silicon", IBM J. Res. Develop., Vol. 23, No. 4, pp. 376-385, July 1979
- [2] E. R. Brown, "RF-MEMS Switches for Reconfigurable Integrated Circuits", IEEE Trans. Microwave Theory Tech., Vol. 46, No. 11, pp. 1868-1880, Nov. 1998
- [3] J. J. Yao, "RF MEMS from a device perspective", J. Micromech. Microeng. Vol. 10, 2000 pp. R9-R38
- [4] D. Hah, E. Yoon, and S. Hong, "A Low Voltage Actuated Micromachined Microwave Switch using Torsion Springs and Leverage", 2000 IEEE MTT-S Digest, pp. 157-160
- [5] S. P. Pacheco, L. P. B. Katehi and C.-T. Nguyen, "Design of Low Actuation Voltage RF MEMS Switch", 2000 IEEE MTT-S Digest, pp. 165-168
- [6] K.M. Strohm, C.N. Rheinfelder, A. Schurr, J.-F. Luy , „SIMMWIC Capacitive RF Switches“, 29th. European Microwave Conference, Munich 1999, Vol. I, pp. 411-414
- [7] D. Pilz, K. M. Strohm, J.-F. Luy, "SIMMWIC-MEMS 180° Switched Line Phase Shifter", 2000 Topical Meeting on Silicon Monolithic Integrated Circuit in RF Systems, 26th - 28th April, 2000, Garmisch, Germany, pp. 113-115
- [8] J. H. Schaffner, R. Y. Loo, A. E. Schmitz, T.-Y Hsu, D. J. Hyman, A. Walston, B. A. Warneke and G. L. Tangoman, S. W. Livingston, "RF MEMS Switches for tunable Filters and Antennas", MOEMS 1999, pp.237-243 Mainz, Germany, Aug. 30.Sept. 1999
- [9] N. Scott Barker, G.M. Rebeiz, "Distributed MEMS True-Time Delay Phase Shifters and Wide-Band Switches", IEEE Trans. Microwave Theory Tech., Vol. 46, No. 11, pp. 1881-1890, Nov. 1998
- [10] H. J. De Los Santos, "Introduction to Microelectromechanical (MEM) Microwave Systems", Artech House, Boston, London 1999